Hydrogeology Journal (2015) 23: 819–836
DOI 10.1007/s10040-014-1223-0

Top-down groundwater hydrograph time-series modeling for climate-pumping decomposition

V. Shapoori · T. J. Peterson · A. W. Western · J. F. Costelloe

Abstract Groundwater time-series modeling has emerged as an efficient approach for simulating the impacts of multiple drivers of groundwater-head variation such as rainfall, evaporation and groundwater pumping. However, a bottom-up approach has generally been adopted whereby the input drivers have been assumed without statistical evidence for their inclusion. In this study, a parsimonious time-series model was adopted which accounts for various drivers and is able to simulate the overall groundwater-head variation. It can also separate the effects of pumping and climate drivers on multi-annual time series of groundwater-level variation. The time-series model consists of a soil-moisture layer to account for non-linearity between rainfall and recharge, as well as different pumping response functions to account for pumping from a single well, lake-induced recharge and the effects of multiple pumping bores. The method was applied to a groundwater-pumping region in south-eastern Australia. The results showed that the model is able to separate the effects of pumping from the effects of climate on groundwater-head variation. However, improved estimation of those influences requires a flexible model structure that can account for spatially varying physical processes within the study region such as the relative influence of single or multiple pumping bores and induced recharge from surface-water bodies.

Keywords Groundwater time series modeling · Climate-pumping decomposition · Statistical modeling · Australia

Received: 12 June 2014 / Accepted: 15 December 2014
Published online: 14 January 2015

Electronic supplementary material The online version of this article (doi:10.1007/s10040-014-1223-0) contains supplementary material, which is available to authorized users.

V. Shapoori (✉) · T. J. Peterson · A. W. Western · J. F. Costelloe
Department of Infrastructure Engineering,
The University of Melbourne, Parkville, VIC 3010, Australia
e-mail: shapoori@student.unimelb.edu.au

Introduction

Groundwater level fluctuation results from many drivers and processes within the catchment (Gallardo 2013; Khan et al. 2007; Konikow and Kendy 2005; Sophocleous 2002); for instance, rainfall recharge, surface-water discharge, phreatic evapotranspiration and groundwater pumping (Konikow and Kendy 2005; Sophocleous 2003; Tularam and Krishna 2009; Zektser et al. 2005). Effective groundwater management, however, often requires identification and separation of these drivers and the prediction of the water level under differing scenarios such as a reduction in pumping. To achieve this, a numerical groundwater model is often built that requires prior assumptions about the hydrogeology and the dominant drivers. This construction of the model based on prior assumptions can make it challenging to objectively identify dominate drivers and processes. In this paper, it is argued that a top-down data-driven time-series modeling approach can objectively provide novel insights into the hydrogeology and drivers within a region. This is demonstrated by the application of a top-down approach to an irrigation region in south-eastern Australia.

The top-down approach involves the data being used to evaluate the necessity of including individual components of the model, thereby identifying the processes supported by the data (Klemes 1983; Sivapalan et al. 2003). Recently, the top-down investigation has been widely advocated in surface hydrology modeling (Atkinson et al. 2002; Farmer et al. 2003; Jothityangkoon et al. 2001; Klemes 1983; Sivapalan et al. 2003; Sivapalan and Young 2005). There, the main causes of spatiotemporal variability of observed data are assessed by systematically evolving the model from simple to more complex structures with additional processes included as required to adequately simulate the system behavior (Atkinson et al. 2002; Farmer et al. 2003; Jothityangkoon et al. 2001). This systematic evaluation was found to be extremely useful in providing insights into the major hydrological processes (e.g. saturation excess flow, evaporation and subsurface runoff) controlling the observed variability (e.g. runoff flow) at different time scale.

For observed groundwater hydrographs, various methods can be adopted to apply such a top-down investigation and quantify the main causes of groundwater

level variations. The simplest of those methods is graphical hydrograph inspection; one application of which is to estimate the pumping radius of influence by estimating the groundwater level decline in surrounding observation bores. Overall, those methods are very simple and usually account for one major impact (e.g. pumping), which make them inappropriate for a top-down process investigation. Numerical groundwater flow modeling with codes such as MODFLOW (McDonald and Harbaugh 1988) is another approach. These models require prior knowledge, or assumptions, of aquifer structure and boundary conditions meaning data-driven assessment of the processes (i.e. top-down investigation) cannot be easily undertaken. Meanwhile, time series models such as ARMAX (Box and Jenkins 1970) are another approach to apply. These models often require less parameter than numerical models and are relatively simple to apply and assess, which make it ideal for the top-down investigation.

However, such a top-down approach has not been applied to time-series groundwater modeling. In the literature, there have been quite a few studies that have used a bottom-up time-series-model approach (Bierkens et al. 1999; Harp and Vesselinov 2011; Obergfell et al. 2013; Peterson and Western 2014; Siriwardena et al. 2011; Von Asmuth et al. 2002; Von Asmuth et al. 2008; Yi and Lee 2004; Yihdego and Webb 2011). Von Asmuth et al. (2002) proposed a specific type of transfer-function noise model adapted for groundwater level simulation. In a bottom-up approach, Von Asmuth et al. (2008) applied the model to the two cases of single and multiple pumping bore extractions. Based on their prior knowledge, they assumed that precipitation, evaporation and pumping are the drivers and the model including all these drivers was used for all bores. In another study, Obergfell et al. (2013) applied the same concept as Von Asmuth et al. (2008), again, assuming that the groundwater head is affected by all drivers (seven pumping bores, precipitation and evaporation drivers) and the most complex model structure was applied to all bores. In an attempt to separate the influence of pumping from climate in these two studies, the calibrated time-series model was also used to decompose the groundwater hydrograph and separate the pumping from climatic influences. While these two studies showed significant advances in the application of time series modeling, neither they, nor any other previous research, independently evaluated the prior assumptions regarding the incorporation of various drivers against observation data (i.e. top down investigation). Furthermore, there was no attempt in either study to further evaluate whether a reliable separation of pumping from climate was achieved.

The main goal of this paper is to use a top-down time-series modeling approach to provide insights into the dominant processes of the study area. In doing so, the time series model proposed by Peterson and Western (2014) model was extended to include a pumping component and tested in a study area in south-eastern Australia. Taking this data driven, top-down approach, the most parsimonious time-series model for each observation bore was identified that (1) is consistent with the local hydrogeology and (2) best simulates the observed groundwater head. The best-performing model structure at each bore was then used as a basis to identify where and when the inclusion of a particular process was warranted and, hence, provides insights into the local hydrogeological processes of importance. Similar to previous studies, each groundwater hydrograph was separated into impacts from pumping and climate. An assessment of the hydrograph separation is made using bores that are not affected by the pumping.

Site description

Climate and hydrogeology

The study area is the Clydebank groundwater subregion of the Gippsland Basin in south-eastern Australia (Fig. 1). This area is relatively flat and surrounded by Lake Wellington in the east and the Avon and Thompson Rivers on the north and south, respectively. Most of the area around Lake Wellington is used for dryland grazing. The area to the west and north along the Avon River has irrigated pasture for dairy. The region is classified as temperate climate with mild winter in the Köppen–Geiger climate classification (Peel et al. 2007).

The subsurface geology of the study area comprises three layers of sedimentary deposits that have accumulated over the period from the early Pliocene to recent times. The top layer is a sequence of clays, sands and gravels with a maximum thickness of 25 m (Hocking 1976; Jenkin 1966). This layer is comprised of prior stream deposits that formed after sea level fell in the late Pleistocene and can be divided into upper and lower subunits (Fig. 2a). The lower subunit contains well-developed beds of coarse sand and gravel, while the upper subunit is composed of finer-grained materials (Jenkin 1966; Nahm 1977). From the lithology data across the whole region, it can be estimated that the upper subunit has a thickness of 4–12 m and the lower subunit is 5–12 m thick. These two subunits are highly connected and respond to climate variation or pumping as one unit (Nahm 1977). The prior stream deposits layer is utilized for private irrigation and is also pumped at public wells to control land salinization. Little is known of the connection of this aquifer to the lakes, irrigation channels or rivers.

The second layer is the Haunted Hills Formation, found at depths of about 15–50 m and consisting of an alluvial outwash fan mainly dominated by sandy clay (Hocking 1976). It has a low permeability and is considered an aquitard between the shallow unconfined aquifer and a deeper confined system consisting of a sequence of Tertiary sediments that reaches a maximum thickness of around 200 m and contributes to regional groundwater flow (Nahm 1977). In this study, only bores within the top unconfined layer are investigated.

 DOI 10.1007/s10040-014-1223-0

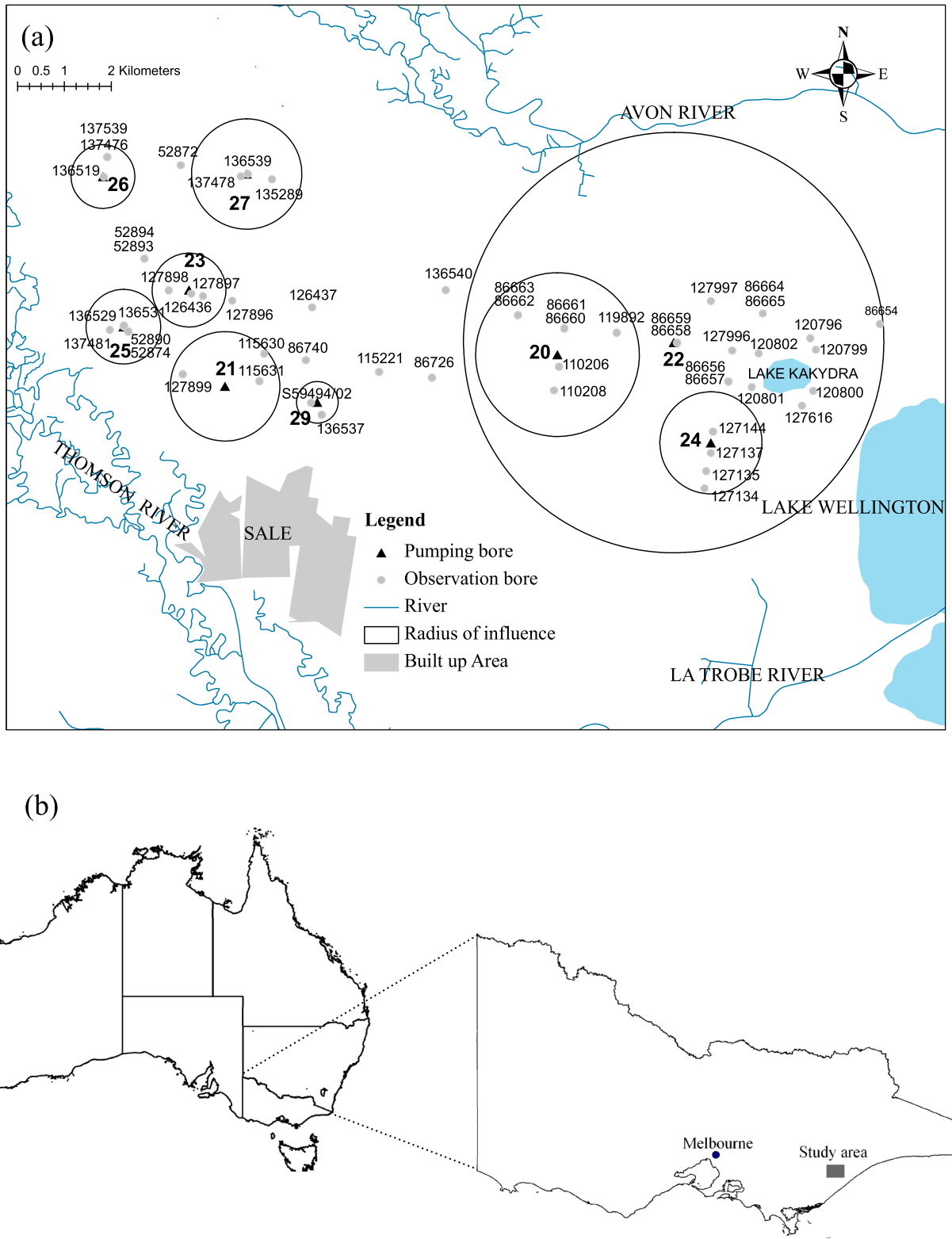

Fig. 1 **a** Locations of observation and pumping bores (with *identification numbers*), **b** Study area location in Victoria, Australia. **a** The *circles* represent the initial estimation of radius of influence from distance drawdown analysis

Land salinity and pumping bores

In this study area, the water table is shallow and saline. To reduce soil salinity, nine pumping bores (Fig. 1) were previously installed to lower the water table. The pumps predominantly operate continuously during winter and spring. Monthly extraction rates were recorded by

DOI 10.1007/s10040-014-1223-0

Victorian Southern Rural Water and are used in the time-series modeling. It is assumed that the monthly extraction volume occurred uniformly throughout each day of the month.

To monitor the effectiveness of the pumping at lowering the water table, 54 observation wells were established and water levels were monitored approximately monthly (Fig. 1). The observation bores were drilled at different times, meaning the observation record length varies. Bores within the ID range of 86,654 to 86,726 have the longest data record, starting in July 1987. Others were drilled and monitored some months before or after the pumping occurred at the closest pumping bore. Detailed information for all observation and pumping bores is available as electronic supplementary material (ESM).

With regard to climatic-forcing data, daily precipitation was obtained from East Sale Airport weather station (Latitude 38.12 °S, Longitude 14.13 °E, Australian Bureau of Meteorology Station 085072) and daily potential evapotranspiration was estimated from the Morton complementary relationship areal model (Morton 1983) using daily values of maximum and minimum temperature, vapor pressure and net radiation from the same station. The annual average precipitation at East Sale airport station and Morton's potential evapotranspiration is estimated at 596 and 1,168 mm/year respectively.

Methods

In the following section, the soil-moisture storage transfer-function-noise model (SMS-TFN) with pumping is outlined starting with the original Von Asmuth et al. (2002) model. Three extensions are then proposed to account for varying saturated thickness, interaction with a lake and pumping from multiple bores. In adopting a top-down approach, each of those proposed model structures is applied to obtain data-based evidence for the most appropriate model structure and, hence, the dominant processes and boundary conditions. Details of the top-down implementation are given in section 'Model implementation'. To aid the assessment of model performance, uncertainty analysis is also undertaken.

The transfer-function noise model

In the Von Asmuth et al. (2002) model, the groundwater level elevation, h_t [L], is the linear sum of three main parts (Eq. 1):

$$h_t = h_t^* + e_t + d \tag{1}$$

where h_t^* [L] is the contribution to head at time step t due to the combined effects of all the represented stresses (i.e. the deterministic part); e_t [L] is the residual series; and d [L] is a constant for the local drainage relative to a reference elevation. Following Von Asmuth et al. (2002), h_t^* can be estimated by assigning an impulse response function to each stressor (e.g. rainfall, evaporation or pumping) to transform the historic forcing to a change in groundwater head (Eq. 2) from d. That is, each impulse response function weights all of the historic forcing and the deterministic change in the groundwater level at time t can be derived by numerically integrating each weighted forcing and summing across all the forcings.

$$h_t^* = \sum_{i=1}^{m} \left(\int_{-\infty}^{t} \theta_i(t-\tau) R_i(\tau) d\tau \right) \tag{2}$$

where θ_i [−] is the predefined impulse response function for stress i; R_i [L] is the input stresses and m [−] is the number of stresses to be modeled.

In applying Eq. (2), Von Asmuth et al. (2002) simulated the climatic stress by inputting the precipitation and potential evapotranspiration as R_i. However, the groundwater head may not respond linearly to climate because of the nonlinearity of interception, runoff and recharge. To account for such nonlinearity, Peterson and Western (2014) extended Von Asmuth et al. (2002) to include a highly flexible soil-moisture model. Depending upon the dynamic sought, the soil-moisture model can have between one and five parameters. Siriwardena et al. (2011) tested all of the models on 620 bores from across Victoria Australia and found the following soil model was the most parsimonious:

$$\frac{ds}{dt} = P\left(1 - \frac{s}{s_{\text{cap}}}\right) - E\left(\frac{s}{s_{\text{cap}}}\right) \tag{3}$$

Here, s_{cap} [L] is a parameter for soil-moisture storage capacity; s [L] is the soil moisture at time t; P [LT^{-1}] is the rate of precipitation and E [LT^{-1}] is the potential evapotranspiration rate. Following Peterson and Western (2014), Eq. (3) was adopted as follows to transform precipitation and potential evapotranspiration for input into the time series model. The precipitation input to the time series was replaced by an estimate of the soil-moisture-free drainage, calculated as $\left(\frac{s}{s_{\text{cap}}}\right)^{\gamma}$, where γ is a parameter for the pore index. The evapotranspiration input was replaced by an estimate of the groundwater evapotranspiration (groundwater ET). This was calculated as $E\left(1-\frac{s}{s_{\text{cap}}}\right)$, that is, potential evapotranspiration minus the modeled soil evapotranspiration. Peterson and Western (2014) undertook the latter replacement to allow the

DOI 10.1007/s10040-014-1223-0

simulation of multi-year groundwater-level decline typical throughout Australia. Biophysically, it can be conceptualized as simulating vegetation groundwater usage only during dry periods; that is, when the soil is very dry. The final time-series model is:

$$h_t = \int_{-\infty}^{t} \left(\frac{s_t}{s_{\text{cap}}}\right)^{\gamma} \theta_{\text{p}}(t-\tau)d\tau - \int_{-\infty}^{t} E_t\left(1-\frac{s_t}{s_{\text{cap}}}\right)\theta_{\text{E}}(t-\tau)d\tau - \int_{-\infty}^{t} Q_t\theta_{\text{F}}(t-\tau)d\tau + e_t + d \quad (4)$$

where E [LT^{-1}] and Q [L^3T^{-1}] are the potential evapotranspiration and pumping rate respectively and θ_{p}, θ_{E} and θ_{F} [−] are the impulse response functions for free drainage, groundwater evapotranspiration and pumping respectively. Originally, the time series model proposed by Peterson and Western (2014) included only the recharge and groundwater evapotranspiration component (i.e. left two integrals in Eq. 4) and in this paper, the third term (pumping component) is added to time series model. Figure 2b shows the conceptual settings considered in the time series model to account for the main processes contributing to the variation in groundwater level. Overall, the three integrals in Eq. (4) represent the influence of the main three drivers, that is free drainage which is dependent on soil moisture controlled by rainfall and evapotranspiration, groundwater ET, and pumping (see Fig. 2b). It should be noted that the model presented here does not consider the possible influence of interaction between drivers and, hence, assumes the drivers are independent of each other. The following sub-sections detail the climatic response functions, θ_{p}, and θ_{E}, and the pumping response function, θ_{F}.

Climatic response function

Von Asmuth et al. (2002) adopted the Pearson type III distribution for the precipitation and evapotranspiration response functions. While it is flexible, Peterson and Western (2014) identified five weaknesses unnecessarily compromising the calibration of the time series model and proposed a more robust distribution. Following Peterson and Western (2014), the impulse response function for climatic stresses was as follows:

When exp (n) – 1>=1:

$$\theta_{\text{p\&E}}(t) = A\frac{t^{\exp(n)-2}\exp(-bt)}{\left(\frac{\exp(n)-2}{b}\right)^{\exp(n)-2}\exp(2-\exp(n))} \quad (5)$$

When exp (n) – 1<1:

$$\theta_{\text{p\&E}}(t) = A\frac{t^{\exp(n)-2}\exp(-bt)-f_{\text{limit}}}{1-f_{\text{limit}}} \quad (6)$$

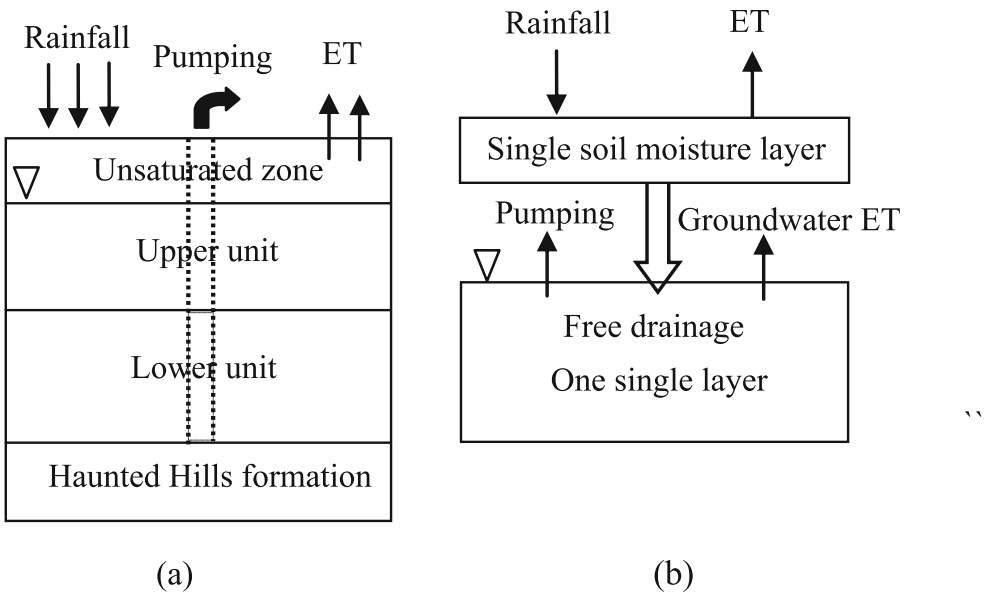

Fig. 2 **a** Conceptualization of the hydrogeology of the study area, **b** Conceptual settings for the model

 DOI 10.1007/s10040-014-1223-0

$$f_{\text{limit}} = t_{\text{limit}}{}^{\exp(n)-2}\exp(-bt_{\text{limit}}) \quad (7)$$

$$t_{\text{limit}} = \min(t)-100 \times 365 \quad (8)$$

where A, b, and n are parameters requiring calibration and $\min(t)$ is the time of the first climate observation; t_{limit} is 100 years prior to the first climate observation date and f_{limit} is the distribution value at 100 years prior to the first climate observation. The A is a scaling parameter. The b and n are the shape parameters, and together they affect the weighting of climate over time. This response function can simulate shapes ranging from Gaussian-like to exponential-like and, hence, enables the simulation of delays between rainfall, recharge and groundwater level response. This delay can represent either the time required for percolation through the unsaturated zone to reach the groundwater at the observation bore or for recharge from more distant locations (e.g. top-hills) to influence the levels at a down-gradient observation site. This implies that the model can account for lateral groundwater flow.

Pumping response function

Unlike the climate response function, the pumping response function can be derived from analytical well hydraulics equations for instantaneous injection or pumping. Numerous such analytical well hydraulics equations have been developed ranging from the Theis equation to those accounting for complexities such as partial well penetration, multiple layer aquifers, sloping beds and isotropic deposits (Kruseman and De Ridder 1994). The inclusion of each additional complexity requires additional parameters, making calibration more challenging and potentially less reproducible. Considering that a top-down approach was adopted, for this study the simplest equation was chosen for the pumping response function; specifically the instantaneous form of the Theis equation, known as Ferris and Knowles' well formula (Eq. 9). In Ferris and Knowles' well formula, the response of the groundwater head (X [L]) to an instantaneous injection or extraction of a volume of water, V [L^3], is described as

$$X = \frac{V}{4\pi Tt}\exp\left(-\frac{r^2 S}{4Tt}\right) \quad (9)$$

Here, T [L^2T^{-1}] and S [−] are transmissivity and storativity of the aquifer around the well respectively, whereas r [L] is the distance from the pumping well to the observation bore. The impulse function is derived from Ferris and Knowles' well formula by replacing the terms $\frac{1}{4\pi T}$ and $\frac{S}{4T}$ in Eq. (9) with parameters α and β respectively (Eq. 10).

$$\theta_{\text{F}}(t) = \frac{\alpha}{t}\exp\left(-\frac{r^2\beta}{t}\right) \quad (10)$$

The distance between the observation bore and pumping well (r) is based on measured data. Ferris and Knowles' well formula has numerous assumptions; for example, the aquifer is homogenous, of infinite areal extent and the saturated thickness is constant. Furthermore, it is limited to a single pumping bore. With regard to the hydrogeology of the study area and the location of pumping bores, some of these assumptions are not valid. The aquifer is unconfined and is only about 10–20 m thick. Considering the observed drawdown is up to 5 m, the assumption of a constant saturated thickness is invalid. Furthermore, the aquifer is locally bounded by the lake (Fig. 1) and some observation bores are likely to be affected by more than one pumping bore. In the following, modifications to the pumping response function are presented to account for the aquifer being unconfined and for the effects of boundary conditions and multiple pumping bores.

Pumping response function with thickness correction inclusion

To account for varying saturated thickness, Jacob (1944) proposed an approximate correction to pump test drawdown data. Following Jacob (1944), to correct for drawdown effects, the observed drawdown (D [L]) can be corrected (D_{c} [L]; Eq. 11).

$$D_{\text{c}} = D-\left(\frac{D^2}{2l}\right) \quad (11)$$

where l [L] is the aquifer thickness. A problem is that in the time series modeling, the observed drawdown, D, is unknown while D_{c} is known (D_{c} is the simulated pumping drawdown derived from the pumping (third) component in Eq. (4). Hence, Eq. (11) is rearranged into an explicit equation for D:

$$D = l\left(1-\sqrt[2]{1-\frac{2D_{\text{c}}}{l}}\right) \quad (12)$$

where l is an additional parameter. To apply this correction, the simulated drawdown (D_{c}) was first calculated from the pumping (third) component in Eq. (4) and then used in Eq. (12) to estimate D. D was then used instead of D_{c} for the pumping (third) component in Eq. (4) when calculating the overall head. This correction was tested for all observation bores. For bores with modest drawdown (<2 m), it produced implausible values of saturated thickness (l) often one or two orders of magnitude greater than those from the bore logs.

DOI 10.1007/s10040-014-1223-0

Therefore, the Jacob's correction was only applied to observation bores in which the drawdown was found to be sufficient to justify its inclusion (bores with blue color in Fig. 10).

Pumping response function with boundary conditions

Where surface-water features are hydraulically connected to an aquifer, their impact on heads may need to be included as an aquifer boundary condition. In assessing if Lake Kakydra (see Fig. 1) influences the response of the aquifer to pumping, the pumping response function (Eq. 10) was extended to include a recharge image well to capture the potential effect of the lake (Ferris 1959).

$$\theta_{F2}(t) = \frac{\alpha}{t}\left(\exp\left(\frac{-r^2\beta}{t}\right) - \exp\left(\frac{-r_r^2\beta}{t}\right)\right) \quad (13)$$

where r_r [L] is a constant for the distance between the image well and the observation bore and it was set to twice the distance from the observation bore to the center of Lake Kakydra. Considering Lake Kakydra is ephemeral and adjacent to the perennial, and significantly larger, Lake Wellington, the image well distance is obviously an approximation. Trials were conducted where r_r was treated as an additional model parameter and derived from calibration. However, implausibly large values for r_r were obtained, which was probably due to the low sensitivity of the parameter.

Response function for multiple pumping bores

The study area contains nine pumping bores. Graphical estimation of their radius of influence indicated that observation bores near pumping bores 20 and 24 may also be influenced by pumping from bore 22 (see Fig. 1). As in pump test analysis (Driscoll 1986; McWhorter and Sunada 1977), the drawdown from multiple pumping bores can be simulated within the time-series model by superimposing response functions for each pumping bore. In this study, this approach was applied to pumping bores 20 and 22 to account for the influence of pumping on observation bores near pumping bore 20 and also to pumping bores 22 and 24, for observations near bore 24. Depending on the assumptions made, this could require two additional model parameters (i.e. α, and β in Eq. (10) for each pumping bore; however, in keeping with the top-down approach of the paper and to minimize the parameters, transmissivity and storativity were assumed to be homogenous within the radius of the influence of each pumping bore. The assumption of homogeneity is consistent with a typical assumption made in pumping testing and the overall top down approach. Obviously, there would be some degree of heterogeneity in this study area but, with limited data, it is not possible to characterize the heterogeneity of the aquifer. Given that model parameters are estimated based on available data, an assumption like homogeneity is pragmatically necessary.

Model implementation

Top-down modeling approach

Four components to the time-series model account for various complexities—groundwater evapotranspiration, time-varying saturated thickness, recharge boundaries, and multiple pumping bores. These model components may or may not be required in a parsimonious model of any given well in the study area. In applying these components, a top-down approach was adopted whereby each component was applied to each observation bore to assess if there was statistical evidence for its inclusion. This approach used the following steps:

1. The inclusion of groundwater evapotranspiration in the time-series model was assessed by applying models with and without the groundwater evapotranspiration component in Eq. (4). In this step, it was assumed that each observation bore is only affected by the closest pumping bore and thickness correction was applied. The results for those two models (with and without groundwater evapotranspiration) were compared and the best one was selected. To assess the model performances, two different criteria were used. The first is the Akaike information criterion with correction (AIC_C; Burnham and Anderson 2004), which penalizes less parsimonious models and is specifically designed to compare models with different numbers of parameters. The second is the coefficient of efficiency (COE; Nash and Sutcliffe 1970) commonly used to assess the performances of hydrological models.
2. For preliminary identification of observation bores likely to be influenced by either multiple pumping bores or a recharge boundary (i.e. lake Kakydra in this study), the distance drawdown analysis method (Driscoll 1986) was used. For each pumping bore, a linear trend-line was fitted between the drawdown at an observation bore (defined as the difference between water level before pumping and the lowest water level after pumping commenced) and the logarithm of the distance of that bore. This was then extrapolated to define a distance producing a 0.1 m drawdown.
3. For bores identified in step two, a further assessment of the evidence for the inclusion of either multiple pumping bores or the lake recharge boundary was undertaken. For those observation bores potentially impacted by multiple pumping bores, the time series model was applied using multiple pumping bores and then compared with the results of a model with only the closest pumping bore included. The model with the best model performance was then selected as the model for that observation bore. For those bores where the lake was within the radius of influence, a similar procedure was applied, whereby models were developed with and without the inclusion of an image well

DOI 10.1007/s10040-014-1223-0

representing the lake and the best performing model was chosen. Since the inclusion of an image well or multiple pumping bores does not change the number of model parameters, only the COE was used for the model performance assessment. The main criterion for the inclusion of an image well or multiple pumping bores at each bore was an improvement in the COE.

Times-series calibration

Following Von Asmuth et al. (2002), in calibrating the time series model, first, the residuals at all observation time points are calculated as:

$$e_t = h_{\mathrm{obs},t} - h_{\mathrm{mod},t} \tag{14}$$

where e_t [L] is the residual at time t; $h_{\mathrm{obs},t}$ [L] is the observed groundwater level at time t; and $h_{\mathrm{mod},t}$ [L] is the modeled groundwater level at time t. The serial correlation in e_t is modeled using an auto-regressive lag one model (AR1); which is equivalent to an exponential decay response in continuous time. The innovation series ($v_{(t)}$) is then calculated from the residuals for the current and previous observations as

$$v_{(t)} = e_t - \exp^{-\mu\Delta t} e_{t-\Delta t} \tag{15}$$

Here, e_t [L] is the residual at time t; $e_{t-\Delta t}$ [L] is the residual at the previous time; Δt [T] is the time between the two observations; and μ is a time-series-model parameter defining the decay rate of the AR1 noise model. Finally, a weighted least-squares objective function was calculated based on the squared innovations and minimized with respect to the parameters using a multi-start trust-region Levenberg-Marquardt gradient based algorithm (Fan and Pan 2006; Levenberg 1944; Marquardt 1963) in which the number and parameter location of the multiple starts were obtained from the eigenvalue approach of Tu and Mayne (2002). In minimizing the innovations, a split sample approach was adopted, whereby the earliest 70 % of the observation record was used for the calibration and the latest 30 % for predictive evaluation. Given that observation record lengths vary, the length of calibration period also varies between observation bores.

Uncertainty analysis

Since the proposed time-series model is sometimes non-linear around the optima, in this study, the non-linear Markov Chain Mont Carlo method (MCMC) was used to estimate uncertainty intervals using the DREAM algorithm. DREAM runs several chains in parallel with initial parameter sets from a prior distribution and then in each chain, new candidate parameter sets are derived based on genetic evolution (Smith and Marshall 2008; Vrugt et al. 2008, 2009). The only algorithm setting that needs to be specified by the user is the number of chains and this was set to the number of parameters being fitted. A total of 500,000 runs of the model were performed using DREAM with independent uniform prior parameter distributions. The prior distribution ranges are detailed in Table 1. The last 10 % of samples in each chain were used to obtain the posterior cumulative distribution functions (CDF) for predictions and parameters and the uncertainties were represented by the 5th and 95th percentiles. These uncertainty estimates only include the influence of parameter uncertainty.

Following Vrugt et al. (2009), to add the remaining unexplained errors to the uncertainty estimation, for each simulation (h^i, i=1, 2,…,j), a normal random error with zero mean and variance of the residual corresponding to each simulation $\{\varepsilon^i \sim \mathrm{N}[0,(\sigma_e^2)^i]\}$ was generated and added to the model simulation. The total uncertainty (parameter uncertainty plus the remaining residual error) were then obtained using a similar approach to that explained above for parameter uncertainty estimation.

Results

In the following, the results of the model-structure selection steps are detailed. Then the spatial and temporal performance of each selected model is detailed, followed by the decomposition of each hydrograph into the contributions from climate and pumping.

Top-down model structure identification

Groundwater evapotranspiration

Models with and without groundwater evapotranspiration (ET) were applied to all observations to identify the validity of simulating groundwater evaporation and COE and AICc performance statistics are presented in Fig. 3. For the calibration period, there is no systematic difference in either COE or AICc values for the models with and without groundwater ET (Fig. 3a–b). More importantly, during the evaluation period, the omission of groundwater ET slightly improves the COE (Fig. 3d) and

Table 1 Model parameters and the prior range for uncertainty analysis

Parameter	Prior range
A	0–1
b	0–0.1
n	0–3
α	0–0.1
β	0–0.01
L	0–20
s_{cap}	0–150
γ	0–10
μ	0–1

DOI 10.1007/s10040-014-1223-0

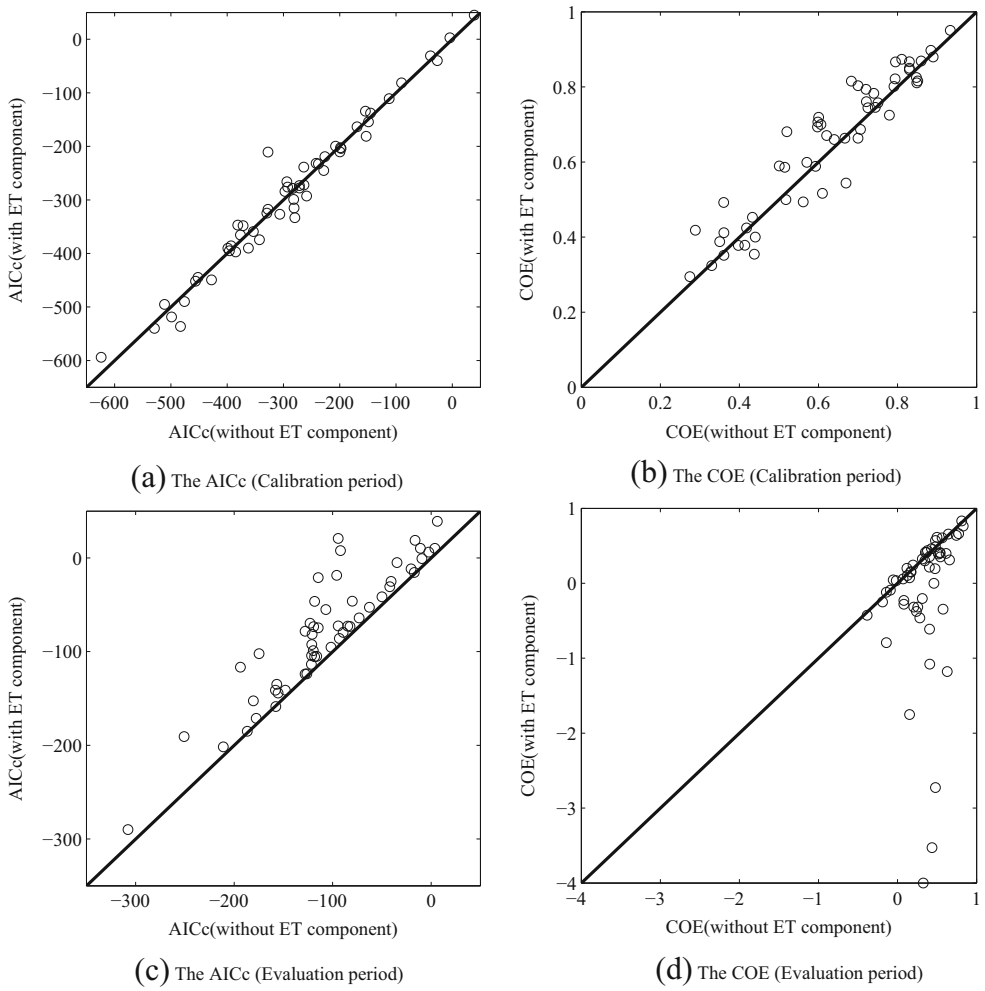

Fig. 3 Comparison of *AICc* and *COE* results between models with the groundwater ET component and models without the groundwater ET component at all the bores in: **a**–**b** the calibration and **c**–**d** evaluation periods. The *1:1 line* is a reference for comparison. In the COE plots (**b**, **d**), points above the 1:1 line are the bores where the model with groundwater ET performs better. In the AICc scatter plots (**a**, **c**), these bores plot below the 1:1 line as lower values of AICc represent better performance

significantly improves AICc (Fig. 3c) at some wells, while at the remaining wells the performance of the two alternate models is comparable. This indicates that the model with the groundwater ET component is sometimes over-fitted during the calibration period as the result of over parameterization. Given that the omission of groundwater ET either led to similar, or improved, model performance in verification, groundwater ET was omitted from all subsequent models.

To determine whether the model with only the free drainage component (i.e. no pumping and groundwater ET) was adequate, the model without groundwater ET was also run with and without pumping at all observation bores. Using the AICc criterion, the results indicated that there was no statistical evidence for the inclusion of pumping at 12 of the 54 observation bores and the simplest model structure (i.e. no groundwater ET and no pumping) was adequate to simulate the groundwater head at those bores. This is an expected result for these 12 bores as these bores are located sufficiently far from the main pumping bore (i.e. >750 m) for the pumping influence to be either too small to detect or zero.

Surface-water boundary effects

For those observation bores where the distance drawdown analysis (Fig. 1) indicated that Lake Kakydra was within the radius of influence, the models were applied with and without a recharge image well and compared using the calibration period COE. Figure 4 shows the change in COE for the seven bores investigated. It shows that at all seven bores the inclusion of a recharge image well improved the model performance. The improvements were not uniform and appear spatially correlated, suggesting regions between pumping bore 22 and Lake Kakydra that are more significantly influenced by pumping-induced lake recharge.

To illustrate the improved model performance from inclusion of the recharge image well, Fig. 5 presents the observed and two simulated hydrographs for bore 86,659.

 DOI 10.1007/s10040-014-1223-0

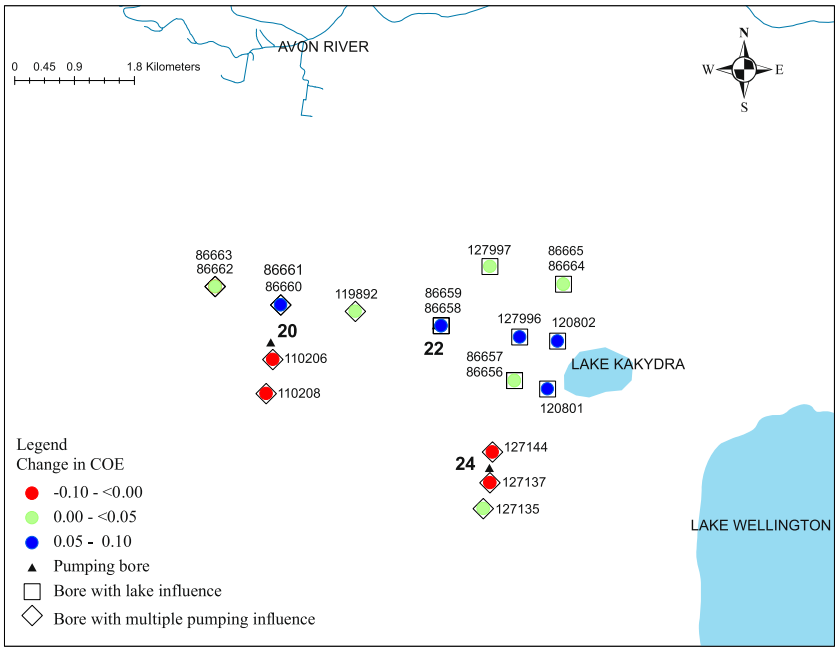

Fig. 4 Change in calibration performance for observation bores (shown with identification numbers) which are either influenced by multiple pumping bores or Lake Kakydra. (Note: change in COE>0 denotes an improvement in the performance of the model from adding multiple pumping wells or the lake.)

It shows that the inclusion of the image well produced a notable improvement over several consecutive points in the fit with the observed hydrograph following the commencement of pumping (1996–1997). For bore 86,659, the root mean square error (RMSE) was 0.49 and 0.60 m in calibration and 0.91 and 1.04 m in evaluation period respectively for the model simulations with and without an image well (i.e. lake). This is an overall improvement of 18 % in calibration and 12 % in evaluation periods when an image well is included in the model structure.

Multiple pumping bores

Distance drawdown analysis showed that eight observation bores need to be assessed for the inclusion of two pumping bores in the model (Fig. 1). Figure 4 presents the change in calibration period COE from the inclusion of a

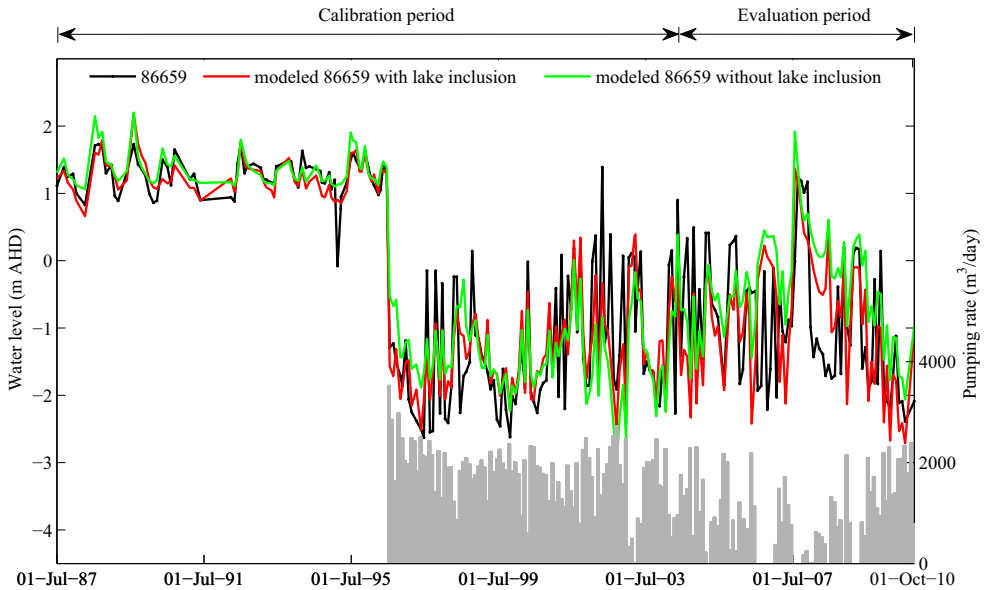

Fig. 5 Effect of lake inclusion for observation bore 86,659. The *black line* is the observed water level. The *red line* denotes the model with lake inclusion. The *green line* is the model without lake inclusion

 DOI 10.1007/s10040-014-1223-0

second pumping bore. It shows that at four of eight bores the COE declined with the inclusion of a second pumping bore (i.e. pump 22), while at four bores COE improved by up to 0.1.

To illustrate the improvement from the inclusion of pump 22 in the simulations, Fig. 6a shows the observed and modeled hydrographs for bore 86,660 and Fig. 6b–c shows extraction rates at pumps 20 and 22 respectively. The most notable improvement from the inclusion of pumps 20 and 22 in the simulation occurs from September 1994 to July 1997. During the first 22 months of this period, only pump 20 was operating. Additionally, during this period, neither model with a single pumping bore adequately simulated the gradual drawdown. After July 1997, Fig. 6a shows less difference between the models, which could be due to poorer model performance after July 1997 or, more likely, the moderate correlation (0.56) between pumping rates in bores 20 and 22 resulting in compensating influences when only one pumping bore is included.

Returning to Fig. 4., three of the four bores (bore 119,892, nested bores 86,660 and 86,662) showing an improvement appear spatially clustered with those bores having a notable improvement, with the inclusion of the image well, while the four bores showing degraded performance with the inclusion of pump 22 are all located to the south. Additionally, three of the four bores (bores 110,206, 127,137 and 127,144) with degraded performances in the south are located close to the main pumping bores (<300 m). For bore 110,208, the degraded performance is possibly due to the lack of water level observation prior to pumping at bore 22, which is in contrast to bore 86,660, which was observed prior to pumping at bore 22. These results suggest that the degradation of model performance for the four bores might be due to either different lithology south of pumping bores 20 and 24 compared with the area to the north of those bores, or more likely, the proximity of these bores to the main pumping bores.

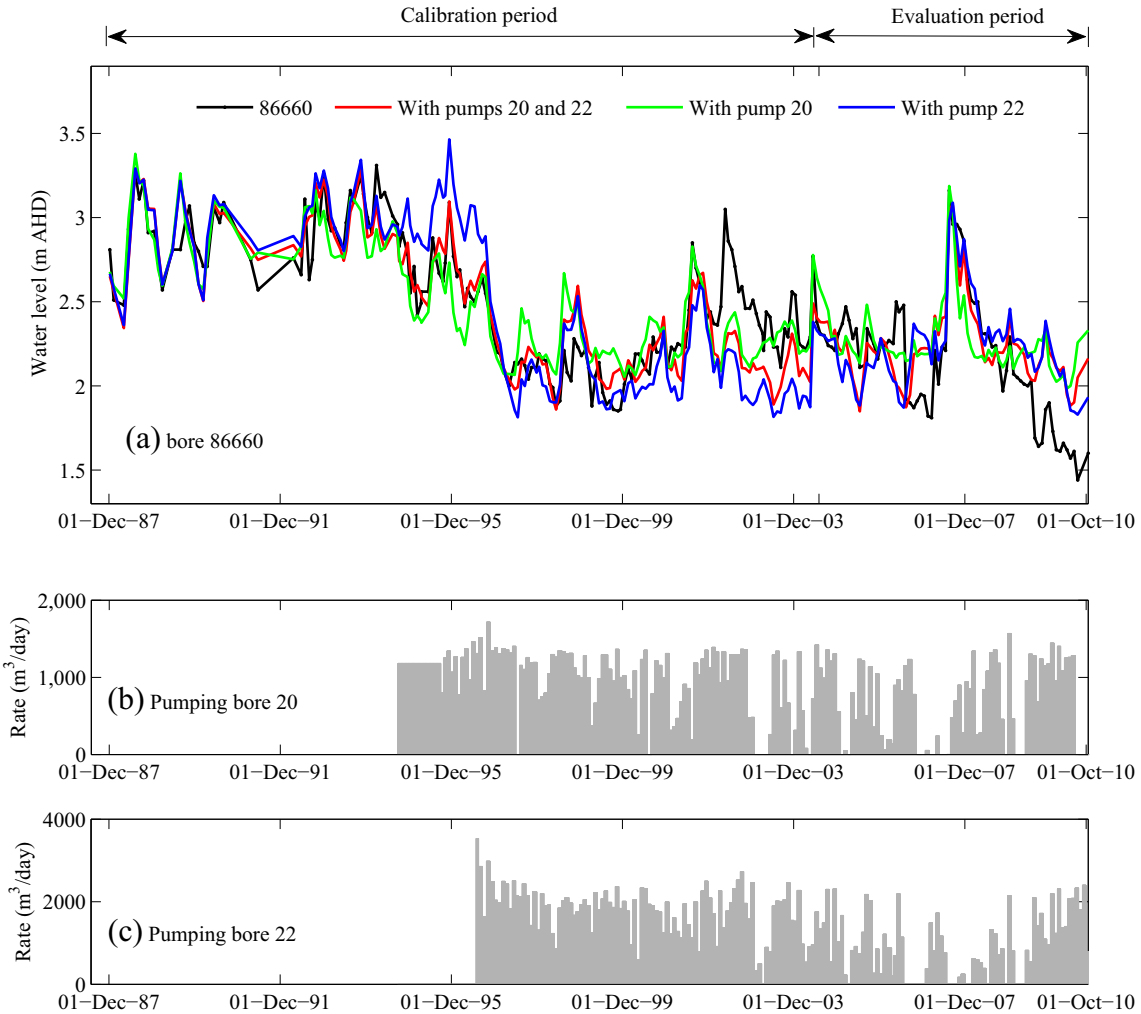

Fig. 6 **a** Multiple bore simulation for observation bore 86,660. The *black line* is the observed water level. The *red line* denotes the model with both pumping bores included. The *green line* is the model with only pumping bore 20. The *blue line* is the model with only pumping bore 22. **b** The rate of pumping for the pumping bore 20 (*the closest one*). **c** The rate of pumping for pumping bore 22 (*the second closest one*)

DOI 10.1007/s10040-014-1223-0

Model performance

Model performance across the study area

To summarize the final model performance for all observation bores, Fig. 7 shows a map of the final calibration and evaluation COEs. With regard to observation bores closest to the pumping bores, it is evident that the chosen model has good COE values (between 0.5 and 1) during the calibration period. However, in the evaluation period, there is an overall degradation in the performance of the model, which is significant in some bores (e.g. nested bores 86,658). As the pumping drawdown declines, other unknown factors can influence the groundwater head and, thus, affect the performance of the model. For instance, the model does not perform well during both calibration and evaluation periods for some

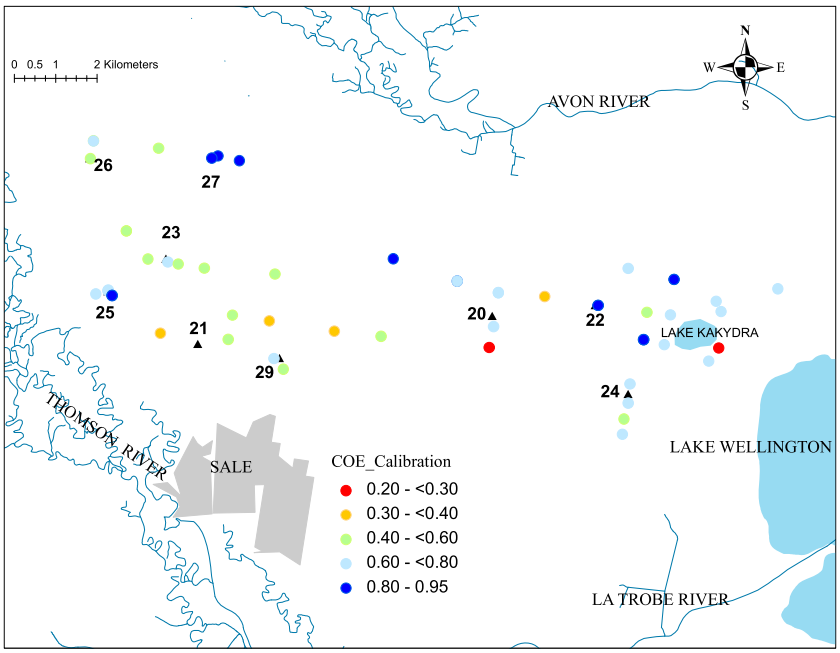

(a)

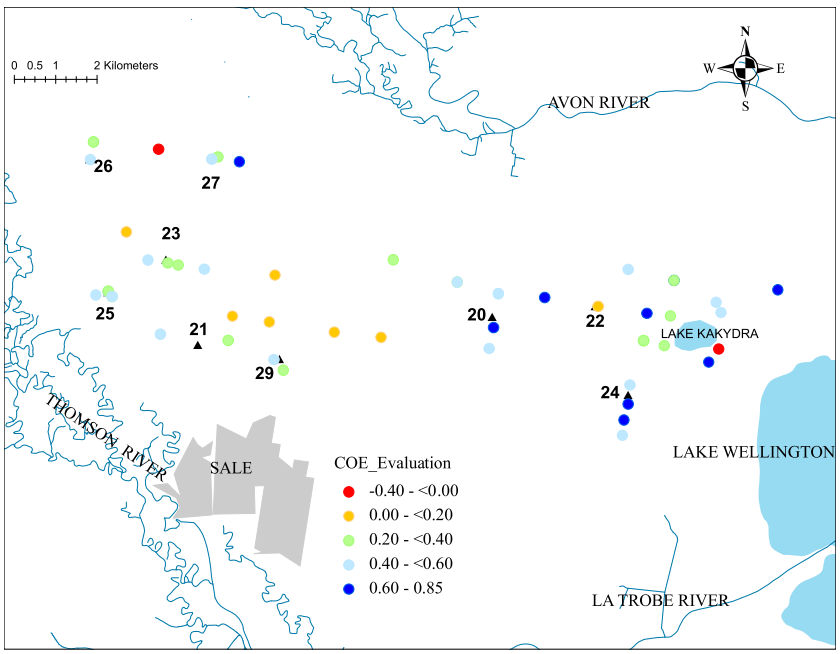

(b)

Fig. 7 The model COE during **a** calibration and **b** evaluation

DOI 10.1007/s10040-014-1223-0

bores that lie on the west side of the area (specifically the region between pumping bores 23, 21, and 29).

Temporal performance and uncertainty

To explore the temporal performance of the modeling, Fig. 8 shows the observed and modeled hydrographs for four bores that represent a range of model behavior. Figure 8a–b shows results for bores within 50 m of a pumping bore and Fig. 8c–d shows results for bores found to be best simulated using only climate forcing. The estimated prediction uncertainty (arising from parameter uncertainty and remaining error) is also presented for the bores in Fig. 8.

For those bores simulated with pumping, Fig. 8a–b shows good agreement between the observed and modeled hydrographs during both the calibration and evaluation periods. For those bores only including climate forcing,

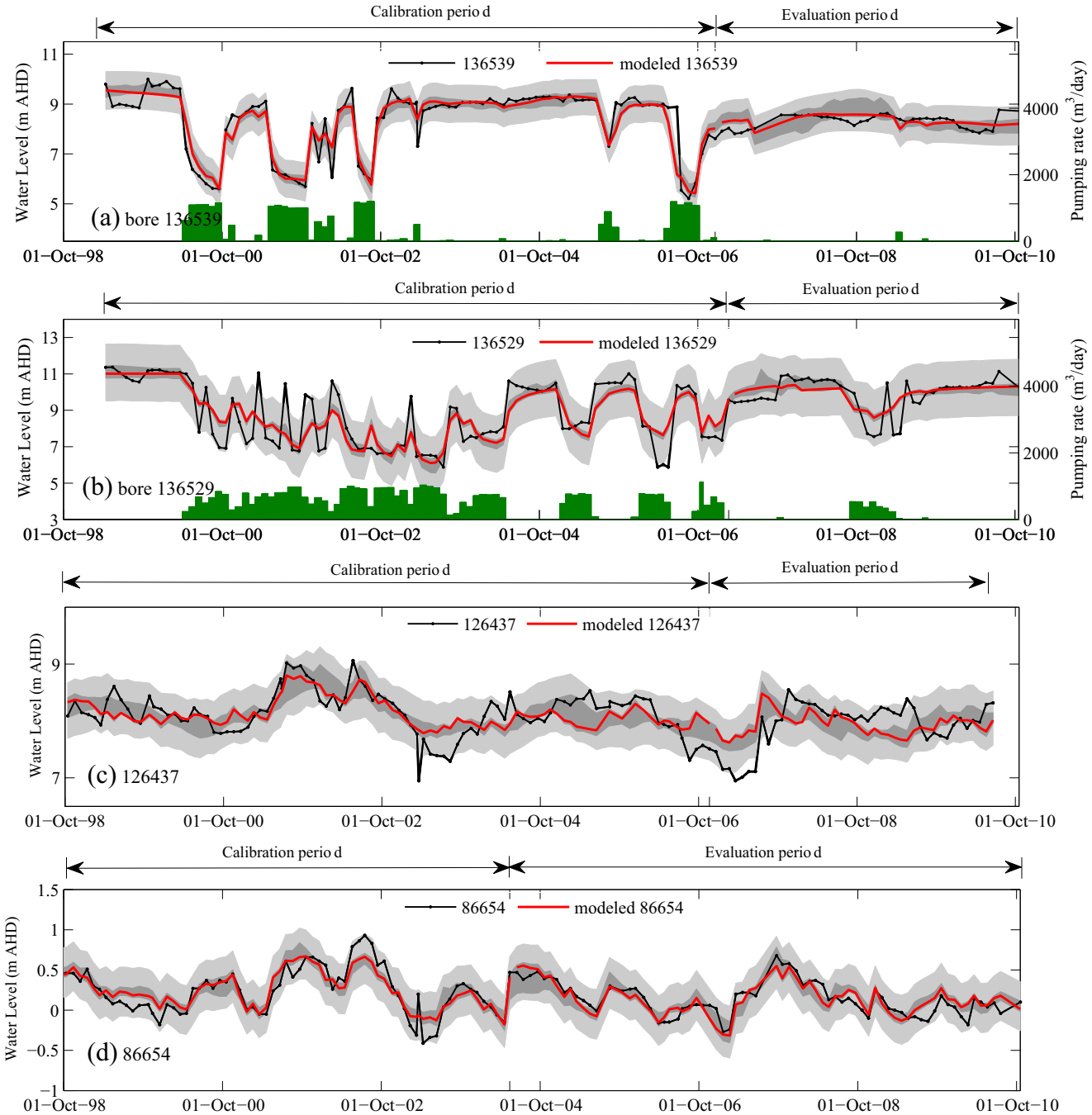

Fig. 8 Observed (*black line*) and modeled groundwater levels (*red line*) for bores **a** 136,539, **b** 136,529, **c** 126,437, **d** 86,654. The *dark green color bars* (**a**–**b**) represent pumping rate. The *dark grey* area represents the 90 % uncertainty interval due to parameter uncertainty, while the *light grey* region shows the additional spread due to remaining residual error. Bore 86,654 is shown *between Oct 1998 and Oct 2010* to make it consistent with other record periods

DOI 10.1007/s10040-014-1223-0

Fig. 8c shows the model performs adequately until October 2002, after which performance declines and is particularly poor during the two periods with lowest head in July 2003 and Oct 2006. This poor performance for that period does not appear to be related to any deficiency in the climate component of the model, as other nearby bores such as bore 86,654 (Fig. 8d), are modeled well with only the climate component. In addition, prior to October 2002, the 1-month serial correlation of residuals was 0.4, after which the serial correlation increased to 0.8. The residual series after October 2002 also showed two periods (March 2003 to Jan 2004 and June 2006 to Oct 2007 in Fig. 8c) in which the model was not able to replicate the drawdown and, thus, the residuals were relatively high, which suggests that after October 2002 an unaccounted-for process has been influencing bore 126,437. This unaccounted process may be unmetered private pumping, which is known to be occurring in this area.

The uncertainty bounds in Fig. 8 show that when the total modeled uncertainty (parameter uncertainty plus the remaining residual error) is accounted for, the bounds capture most observed data. In contrast, fewer observations fall within the parameter uncertainty bounds and there are observed water level dynamics that are consistently outside the parameter uncertainty estimation (see Fig. 8b October 2000 to October 2002). To further assess the uncertainty bounds, the coverage was calculated as the percentage of observations within either the parameter or total uncertainty bounds for the bores shown in Fig. 8, as well as all other observation bores during the calibration period. The results showed that the coverage due to parameter uncertainty varied between 20 and 75 %, with the median being 36 %, while the coverage due to the total uncertainty varied between 87 and 98 % with the median being 93 %. This is consistent with the 90 % uncertainty bounds used; however, the contribution of the residual error term appears to be significant and parameter uncertainty alone significantly under-estimates the total uncertainty.

Hydrograph decomposition

Decomposition at selected bores

One of the main strengths of the proposed model is its ability to separate the effects of the main drivers: climate and pumping. Two examples are presented to show the effectiveness of the proposed model in separating the pumping influence from climate (Fig. 9). To illustrate this separation, the calibrated model was run with only the climate component through the whole available data time series, and then again with both the climate and pumping components. Figure 9a–b shows that the pumping rapidly affects groundwater head for the period July 1996 up to July 1997. At the start of this period, the groundwater head declined gradually and reached its lowest value of −1.22 (m relative to the Australian Height Datum, AHD) for bore 86,656 in Fig. 9a and −1.89 (m AHD) for bore 127,144 in Fig. 9b. A simple interpretation might conclude that this entire water-level drop is the result of pumping; however, from the model simulation with only climate, it is clear that after July 1996, the groundwater head also started to decline gradually in response to climatic influences and, hence, the observed groundwater head decline is due to both pumping and recession after a large recharge event.

To evaluate the hydrograph decomposition, the simulations derived without pumping were compared with an observation bore not influenced by pumping (see Fig. 9a–b). It can be seen that observed data from bores 86,654 and 86,656 and the modeled 86,656 data follow the same trend before pumping occurred with similar responses to recharge events and subsequent gradual declines (Fig. 9a). For the period after pumping, interestingly, this trend continues between observed 86,654 data and the modeled climate-only response of 86,656. To quantify this similarity statistically, the correlation coefficient was calculated; the results also showed a strong relationship (correlation coefficient of 0.62) between bores 86,654 and 86,656 before pumping, which continues to be strong (correlation coefficient of 0.75) between the modeled climate responses of 86,656 and bore 86,654 during pumping. While there are no observation data available before pumping for bore 127,144 (Fig. 9b), it is again clear that observed data from bore 127,137 found not to be influenced by pumping and the modeled climate-only response of 127,144, follow the same trend and respond similarly to recharge and subsequent declines during the pumping period. These comparisons provide important evidence suggesting that the climate signal is well predicted and hence the difference between the climate-only model and the observation bore is a reliable estimation of the pumping effect.

Estimated drawdown across the study area

The prior subsection provided evidence that the decomposition of the simulated hydrograph is consistent with independent observations. In this section, this decomposition was undertaken for all bores and Fig. 10 summarizes the maximum drawdown from pumping at each observation bore. The adequate decomposition can be derived only for those bores in which good model performances are achieved. For those bores with poorer model performances (e.g. those influenced by unmetered pumping or additional recharge from lakes), some errors will be included in the decomposition of the simulated hydrograph. The estimated drawdown within 300 m of pumping bores is between 2.0 and 5.2 m and, as expected, drawdown decreases with distance from pumping bores.

Discussion and conclusions

Top-down approach to time-series modeling

In this paper, a systematic, top-down approach was applied to identify the most parsimonious model structure at each observation bore. This approach identified where and when the inclusion of a particular process was

DOI 10.1007/s10040-014-1223-0

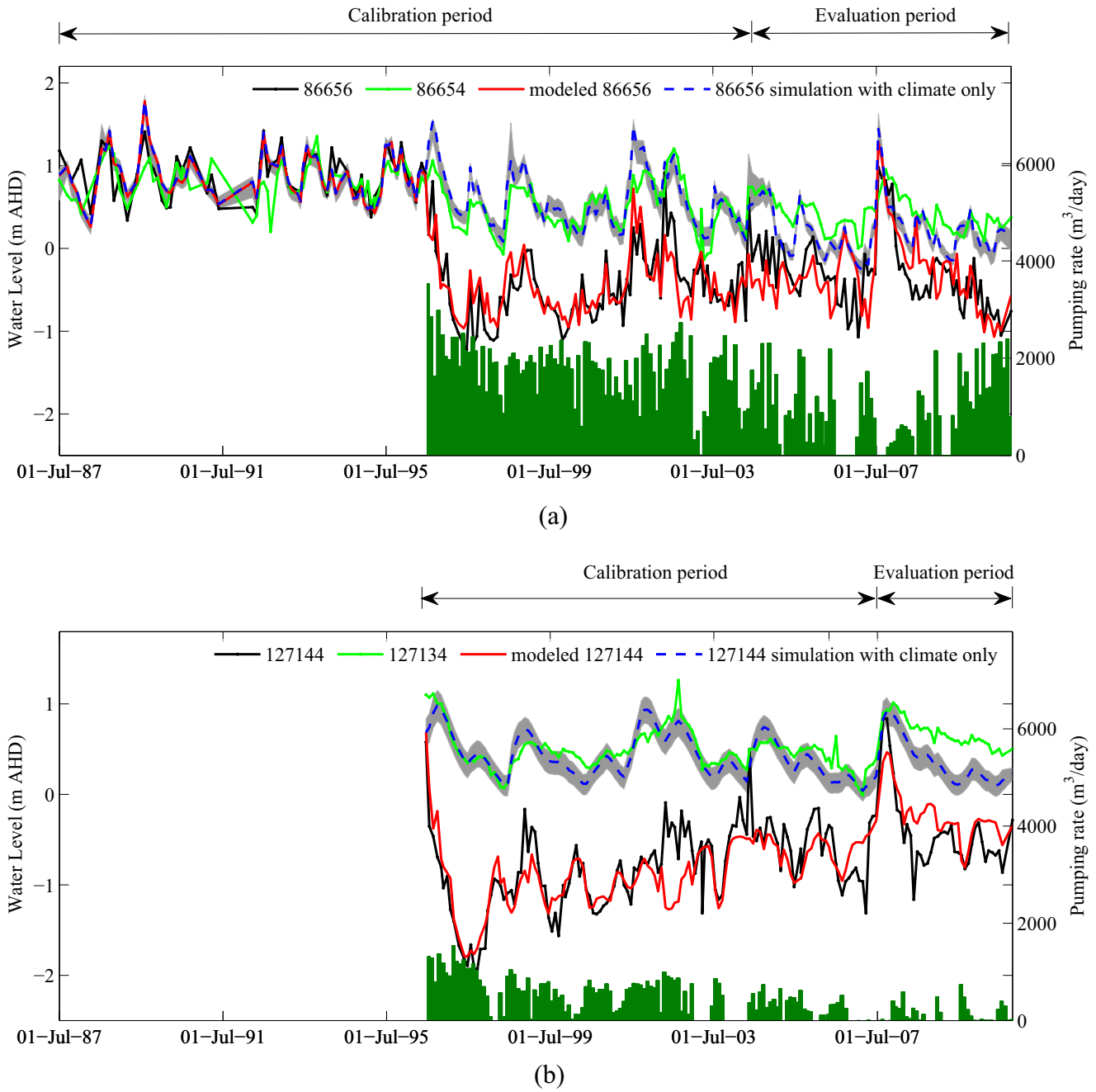

Fig. 9 Modeled (*red line*) and simulated hydrographs with the climate component only (*dashed blue line*) for the observation bore 86,656 (**a**) and 127,144 (**b**). The *light green line* is observation bore 86,654 (**a**) and 127,134 (**b**). The *dark green color bars* represent pumping rate. The *dark grey* area represents the 90 % uncertainty interval due to parameter uncertainty for the model run with only the climate components. Note that for clarity, uncertainty for observation bores and the additional spread due to remaining residual error are not presented

warranted, which provided insights into the hydrogeological processes of importance. In the following, two examples are detailed.

Evaluation of the groundwater evapotranspiration component in the model demonstrates the advantage of top-down investigation. In recent groundwater time-series studies, such as Von Asmuth et al. (2008), Obergfell et al. (2013), Yihdego and Webb (2011) and Peterson and Western (2014), groundwater evapotranspiration was assumed to be one of the major processes prior to modeling, with no evaluation of the significance of that driver. In this study, the model with a groundwater evapotranspiration component performed better during the calibration period for some observation bores but did not adequately simulate the groundwater head during the evaluation period (Fig. 3). This indicates that the component is redundant in the study area, resulting in a risk of over fitting the model during calibration. One reason why the groundwater evapotranspiration is not a major

DOI 10.1007/s10040-014-1223-0

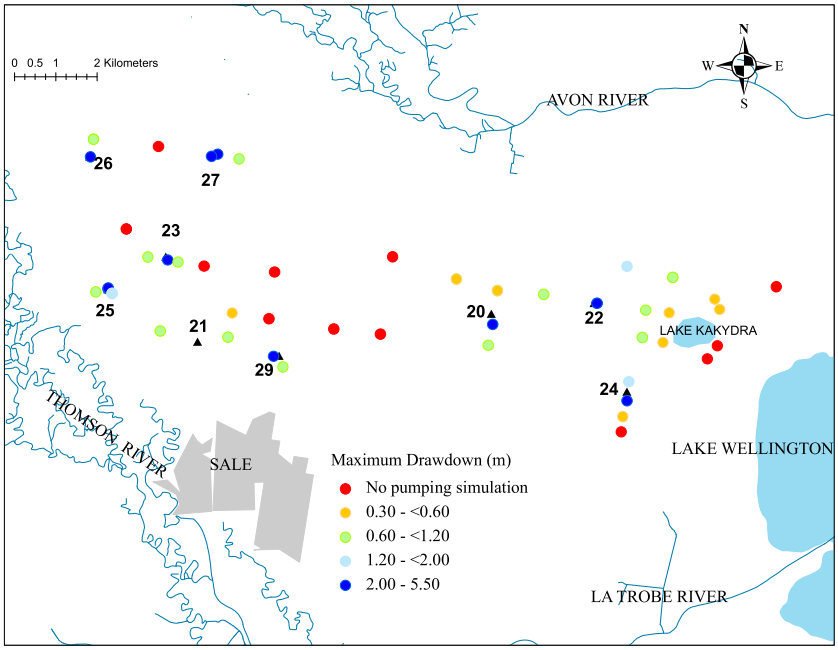

Fig. 10 The maximum drawdown derived from the pumping component of the model for the pumping periods

driver may relate to local conditions; that is, in the study area, the groundwater is highly saline and the vegetation is dominantly shallow-rooted and, therefore, phreatic uptake of water by the vegetation is unlikely to be a significant flux. It could be argued that the model does not account for interaction between the drivers, and, given the changes associated with the introduction of pumping, this could be concealing an effect of evapotranspiration. However, this cannot be the main factor since for those bores not influenced by pumping (e.g. bores 86,654 or 115,221) and the model still best simulated the groundwater hydrographs without groundwater ET.

The top-down approach was also used to evaluate the need for including multiple pumping bores. While Obergfell et al. (2013) also used the superposition of multiple pumping bores, in their study the inclusion of seven pumping bores was decided prior to modeling and not further evaluated. In contrast, the result of this study showed that accounting for an extra pumping bore does not necessarily improve the model performance (Fig. 4). It was shown here that there was a region where an additional pumping bore does not produce benefits. This highlights the importance of the top-down approach to facilitate the delineation of such regions and to potentially provide insights into local conditions (e.g. soil heterogeneity) with few prior assumptions.

Inclusion of an additional source of recharge from the lake

The application of a top-down approach to time series modeling of a well-field allows the investigation of local spatial influences on groundwater responses. In this study, the influence of additional sources of recharge from nearby water bodies (e.g. Lake Kakydra, Fig. 4) due to pumping-induced drawdown was evaluated and this is the first time where an additional source of recharge is explicitly included in the time series model. The results showed that improvements in the model performance metrics due to inclusion of the lake are modest, but when the hydrographs are considered in detail, there are consecutive improvements for specific periods (e.g. following the commencement of pumping, Fig. 5), supporting the potential existence of some influence from the lake.

The proposed pumping response function that accounts for a lake boundary condition, while performing acceptably in this situation, should be used with caution due to the assumptions made. These are that the recharge source fully penetrates the aquifer (at least in terms of determining the underlying head) and the river, channel or lake is sufficiently long so that the solution is independent of the length of the recharge source. In this study, the second assumption is not satisfied as the lake has limited extent in the direction perpendicular to the pumping flow. This limitation is accepted at this stage given that no image well configurations have been developed to include the recharge effect of a finite water body despite several analytical image well configurations for mixtures of recharge and barrier boundaries (Kruseman and De Ridder 1994). Furthermore, no image well configuration was known that could account for variable lake stage height. To account for the lake recharge influence, one possibility would be to model the lake as a recharge boundary with a circle-like shape and

 DOI 10.1007/s10040-014-1223-0

use the block-wise constant recharge function presented in Bruggeman (1999) to describe the response of the aquifer to a constant flux of recharge within a specific area. However, applying such an approach requires definition of the lake recharge rate. The coupling of a time-varying lake recharge rate with a time series model is the subject of future research.

Evaluation of pumping separation from climate

One of the important aspects of the time series model is its ability to decompose the groundwater hydrograph and quantify the influences of individual drivers. In previous studies (e.g. Von Asmuth et al. 2008 and Obergfell et al. 2013), hydrograph decomposition to climate and pumping was undertaken but the reliability of the separations was not assessed. There appears to have been an assumption that a good fit to the hydrographs would result in reliable decompositions. This assumption has been shown to be questionable (Shapoori et al. 2011). In this study, a simple approach providing a reasonable check of the hydrograph separations was an option. This was done by comparison of decomposition against independent bore data (Fig. 9), which was possible due to the configuration of the study area and wells. The results indicated a good agreement between the bores uninfluenced by pumping and the decomposed hydrograph and, hence, provides considerable confidence that adequate separation has been achieved. An understanding of the key drivers of head variation and a reliable approach for separation of pumping from climatic influences are essential for better management of groundwater resources. The results in this study indicate that the top-down approach is able to provide significant insight into the importance of different drivers and the resulting time series models provided reliable separations.

The value of time-series modeling and other approaches

This paper has demonstrated that the adoption of a top-down modeling approach can improve model performance and, just as importantly, provides insights into hydrological processes, the hydrogeology, and unmetered groundwater usage, with minimal prior assumptions. Clearly, there are some deficiencies in this statistical approach to groundwater modeling that require further research, namely the limitations of the adopted analytical drawdown functions and the image well equations. Despite this, it has been demonstrated that time series modeling is a valuable tool that can be used in place of, or in conjunction with, other methods such as analytical simulation or numerical modeling to efficiently provide novel insights.

Acknowledgements The authors are grateful for the financial support received from the Australian Research Council (grant number: LP0991280), the Department of Sustainability and Environment, Victoria, Australia; the Department of Primary Industries, Victoria, Australia; and the Bureau of Meteorology, Australia. The authors also thank Mr. Andrew Harrison and Mr. Terry Flynn for providing the pumping data and information on the study area and the anonymous reviewers for their valuable comments

References

Atkinson SE, Woods RA, Sivapalan M (2002) Climate and landscape controls on water balance model complexity over changing timescales. Water Resour Res 38:1314. doi:10.1029/2002WR001487

Bierkens MFP, Knotters M, van Geer FC (1999) Calibration of transfer function-noise models to sparsely or irregularly observed time series. Water Resour Res 35:1741–1750

Box GEP, Jenkins GM (1970) Time series analysis: forecasting and control. Holden-Day, San Francisco

Bruggeman GA (1999) Analytical solutions of geohydrological problems. Elsevier, Amsterdam

Burnham KP, Anderson DR (2004) Multimodel inference: understanding AIC and BIC in model selection. Sociol Methods Res 33:261–314

Driscoll FG (1986) Groundwater and wells. Johnson Filtration Systems, St. Paul, MN

Fan J, Pan J (2006) Convergence properties of a self-adaptive Levenberg-Marquardt algorithm under local error bound condition. Comput Optim Appl 34:47–62

Farmer D, Sivapalan M, Jothityangkoon C (2003) Climate, soil, and vegetation controls upon the variability of water balance in temperate and semiarid landscapes: downward approach to water balance analysis. Water Resour Res 39:1035. doi:10.1029/2001WR000328

Ferris JG (1959) Ground water. In: Wisler CO, Brater EF (eds) Hydrology. Wiley, New York

Gallardo AH (2013) Groundwater levels under climate change in the Gnangara system, Western Australia. J Water Clim Chang 4:52–62

Harp D, Vesselinov V (2011) Identification of pumping influences in long-term water level fluctuations. Groundwater 49:403–414. doi:10.1111/j.1745-6584.2010.00725.x

Hocking JB (1976) Gippsland Basin. In: Douglas JA, Ferguson JA (eds) Geology of Victoria. Geological Society of Australia, Sydney

Jacob CE (1944) Notes on determining permeability by pumping tests under water-table conditions. US Geological Survey, Reston, VA

Jenkin JJ (1966) The geomorphology and upper Cainozoic geology of south-east Gippsland. PhD Thesis, University of Melbourne, Australia

Jothityangkoon C, Sivapalan M, Farmer D (2001) Process controls of water balance variability in a large semi-arid catchment: downward approach to hydrological modeling. J Hydrol 254:174–198

Khan S, Ahmad A, Wang B (2007) Quantifying rainfall and flooding impacts on groundwater levels in irrigation areas: GIS approach. J Irrig Drain Eng 133:359–367. doi:10.1061/(asce)0733-9437

Klemes V (1983) Conceptualization and scale in hydrology. J Hydrol 65:1–23

Konikow LF, Kendy E (2005) Groundwater depletion: a global problem. Hydrogeol J 13:317–320. doi:10.1007/s10040-004-0411-8

Kruseman GP, De Ridder NA (1994) Analysis and evaluation of pumping test data. International Institute for Land Reclamation and Improvement, Wageningen, The Netherlands

Levenberg K (1944) A method for the solution of certain non-linear problems in least squares. Q Appl Math 2:164–168

Marquardt DW (1963) An algorithm for least-squares estimation of nonlinear parameters. J Soc Ind Appl Math 11:431–441

McDonald MG, Harbaugh AW (1988) A modular three-dimensional finite-difference ground-water flow model. US Geol Surv Tech Water Resour Invest, book 6, chap A1. US Geological Survey, Denver, CO

McWhorter DB, Sunada DK (1977) Groundwater hydrology and hydraulics. Water Resources, Littleton, CO

Morton FI (1983) Operational estimates of areal evapotranspiration and their significance to the science and practice of hydrology. J Hydrol 66:1–76

Nahm Y (1977) Groundwater resources in Gippsland. Geological Survey of Victoria, Melbourne

Nash JE, Sutcliffe JV (1970) River flow forecasting through conceptual models, part I: a discussion of principles. J Hydrol 10:282–290. doi:10.1016/0022-1694(70)90255-6

Obergfell C, Bakker M, Zaadnoordijk WJ, Maas K (2013) Deriving hydrogeological parameters through time series analysis of groundwater head fluctuations around well fields. Hydrogeol J 21:987–999

Peel MC, Finlayson BL, McMahon TA (2007) Updated world map of the Köppen-Geiger climate classification. Hydrol Earth Syst Sci Discuss 4:439–473

Peterson TJ, Western AW (2014) Nonlinear time series modeling of unconfined groundwater head. Water Resour Res 50:8330–8355. doi:10.1002/2013WR014800

Shapoori V, Peterson TJ, Western AW, Costelloe JF (2011) Quantifying the impact of pumping on groundwater heads using observation data and advanced time series analysis. Paper presented at the International Congress on Modelling and Simulation, Perth, Australia, Dec 2011, pp 12–16

Siriwardena L, Peterson TJ, Western AW (2011) A state-wide assessment of optimal groundwater hydrograph time series models. Paper presented at the International Congress on Modeling and Simulation, Perth, Australia, Dec 2011, pp 12–16

Sivapalan M, Young PC (2005) Downward approach to hydrological model development. Encycl Hydrol Sci 3:2081–2098

Sivapalan M, Bloschl G, Zhang L, Vertessy R (2003) Downward approach to hydrological prediction. Hydrol Process 17:2101–2111

Smith TJ, Marshall LA (2008) Bayesian methods in hydrologic modeling: a study of recent advancements in Markov chain Monte Carlo techniques. Water Resour Res 44:W00B05. doi:10.1029/2007WR006705

Sophocleous M (2002) Interactions between groundwater and surface water: the state of the science. Hydrogeol J 10:52–67

Sophocleous M (2003) Environmental implications of intensive groundwater use with special regard to streams and wetlands, chap 4. In: Intensive use of groundwater. Balkema, Lisse, The Netherlands

Tu W, Mayne R (2002) Studies of multi-start clustering for global optimization. Int J Numer Methods Eng 53:2239–2252

Tularam GA, Krishna M (2009) Long-term consequences of groundwater pumping in Australia a review of impacts around the globe. J Appl Sci Environ Sanit 4:151–166

Von Asmuth JR, Bierkens MFP, Maas K (2002) Transfer function-noise modeling in continuous time using predefined impulse response functions. Water Resour Res 38:23. doi:10.1029/2001WR001136

Von Asmuth JR, Maas K, Bakker M, Petersen J (2008) Modeling time series of ground water head fluctuations subjected to multiple stresses. Ground Water 46:30–40. doi:10.1111/j.1745-6584.2007.00382.x

Vrugt JA, Braak CFJ, Clark MP, Hyman JM, Robinson BA (2008) Treatment of input uncertainty in hydrologic modeling: doing hydrology backward with Markov chain Monte Carlo simulation. Water Resour Res 44:W00B09. doi:10.1029/2007WR006720

Vrugt JA, Ter Braak CJF, Diks CGH, Robinson BA, Hyman JM, Higdon D (2009) Accelerating Markov Chain Monte Carlo simulation by differential evolution with self-adaptive randomized subspace sampling. Int J Nonlinear Sci Numer Simul 10:273–290

Yi MJ, Lee KK (2004) Transfer function-noise modeling of irregularly observed groundwater heads using precipitation data. J Hydrol 288:272–287. doi:10.1016/j.jhydrol.2003.10.020

Yihdego Y, Webb JA (2011) Modeling of bore hydrographs to determine the impact of climate and land-use change in a temperate subhumid region of southeastern Australia. Hydrogeol J 19:877–887. doi:10.1007/s10040-011-0726-1

Zektser S, Loaiciga HA, Wolf JT (2005) Environmental impacts of groundwater overdraft: selected case studies in the southwestern United States. Environ Geol 47:396–404. doi:10.1007/s00254-004-1164-3